Journal of Power Sources 191 (2009) 433–441

Contents lists available at ScienceDirect

Journal of Power Sources

journal homepage: www.elsevier.com/locate/jpowsour

Improvement of proton exchange membrane fuel cell overall efficiency by integrating heat-to-electricity conversion

Chungang Xie [a], Shuxin Wang [a,*], Lianhong Zhang [a], S. Jack Hu [b]

[a] School of Mechanical Engineering, Tianjin University, Tianjin 300072, China
[b] Department of Mechanical Engineering, The University of Michigan, Ann Arbor, MI 48109-2125, USA

ARTICLE INFO

Article history:
Received 25 November 2008
Received in revised form 12 February 2009
Accepted 13 February 2009
Available online 3 March 2009

Keywords:
Distributed power generation
PEMFC
Exergy analysis
Overall efficiency
Thermal energy conversion (TEC)

ABSTRACT

Proton exchange membrane fuel cells (PEMFCs) have shown to be well suited for distributed power generation due to their excellent performance. However, a PEMFC produces a considerable amount of heat in the process of electrochemical reaction. It is desirable to use thermal energy for electricity generation in addition to heating applications. Based on the operating characteristics of a PEMFC, an advanced thermal energy conversion system using "ocean thermal energy conversion" (OTEC) technology is applied to exploit the thermal energy of the PEMFC for electricity generation. Through this combination of technology, this unique PEMFC power plant not only achieves the combined heat and power efficiency, but also adequately utilizes heat to generate more valuable electricity. Exergy analysis illustrates the improvement of overall efficiency and energy flow distribution in the power plant. Analytical results show that the overall efficiency of the PEMFC is increased by 0.4–2.3% due to the thermal energy conversion (TEC) system. It is also evident that the PEMFC should operate within the optimal load range by balancing the design parameters of the PEMFC and of the TEC system.

1. Introduction

Demand for energy has been rising quickly due to economical development and population growth. More and more fossil fuels are being extracted to meet worldwide energy demands. It is well known that burning fossil fuels contributes to global climate change and environmental pollution and that fossil fuels are limited in their supply [1–3]. Severe environmental problems and the increasing cost of primary energy have motivated worldwide interest in renewable energy technology [4–7]. However, it is difficult for any new technology to quickly achieve the economical feasibility of energy production [8–10]. Many researchers have suggested that better energy conversion methods and improvements in conversion efficiency should be effective ways to deal with energy utilization [1,11].

Electricity is the most well known energy carrier. Energy from coal, crude oil, uranium, flowing water and air, etc. can be distributed to homes or businesses in the form of electricity. Similar to electricity, hydrogen has also been recognized as one potential energy carrier, while a hydrogen fuel cell is believed to be a viable energy conversion device due to its high performance and low negative effects [12,13]. Among the various types of fuel cells, proton exchange membrane fuel cells (PEMFCs) have achieved fast commercial development in recent years due to their inherent qualities: high efficiency, high power density, low operating temperature, fast start-up and responsiveness to load changes. At present, the PEMFC has been successfully applied in various fields such as portable power, transportation, and stationary/distributed power generation [14,15].

A PEMFC acts as a residential distributed power generation with two compelling advantages over conventional power generation: (1) generally, there is a great fluctuation for electricity demand in a community during the course of a day. However, the PEMFC has great ability to respond to the changes of electrical loads and adapts well to the high volatility in electricity demand [16]. Such flexibility in closely matching the supply with instantaneous demand is one of the most important engineering characteristics for a power plant. (2) According to local natural conditions, different kinds of renewable energy such as solar, wind, geothermal heat and biofuel can be exploited to become important providers of fuel for the fuel cell. Thus, diversity of the energy source is beneficial for the fuel cell to adapt well to the regional decentralization of the future energy supply and reduce fossil fuel consumption [17].

In a community or a building, the residents are likely to desire that the local power plant provides not only electricity but also heat. Conventional power plants usually focus on the improvement of electrical efficiency and neglect the disposition of the by-product heat. Most thermal energy is viewed as waste heat and is released into the environment rather than being used for heating, result-

* Corresponding author. Tel.: +86 22 27405564; fax: +86 22 87402173.
E-mail address: shuxinw@tju.edu.cn (S. Wang).

0378-7753/$ – see front matter © 2009 Elsevier B.V. All rights reserved.
doi:10.1016/j.jpowsour.2009.02.048

ing in economic and environmental inefficiencies [18]. As such, the combined heat and power technology has been recognized as a key advantage for the distributed generation application [19,20]. For the PEMFC it is easy to construct a combined heat and power system based on thermal management. Among the heat generated by the PEMFC, one part is necessary to maintain normal operating temperatures of the PEMFC, while the redundant heat is required to be removed during the operation in order to prevent the membrane from dehydration and overheating. The excess heat can be easily collected and transferred to the user by the cooling system of the PEMFC. Therefore, in this way, a combined heat and power fuel cell system will be able to gain improved overall efficiency.

From the view point of energy quality, among the output energy of the PEMFC, electricity is one form of available energy which can be utilized to do useful work. Heat is only partly applicable to perform work, but it is a large portion of the total output energy which is in the range of 40–60% depending on the electrical efficiency of the PEMFC [21,22]. Such heat, even if low quality, i.e., with a small temperature difference (20–60 °C) between source and sink, may still be considered for use in a heat engine to generate more electricity. In this process of energy conversion, an important issue must be observed in that PEMFC usually operates at a temperature of about 70 °C for the sake of safety and stability [23,24]. Such a low temperature makes it difficult to use reaction heat for secondary electricity generation by conventional techniques. However, as a result of the recent development of modern renewable energy conversion technologies, some effective methods can be adopted to extract the low-temperature heat to generate electricity efficiently [8,25]. This article describes a conceptual design for a combined heat and power PEMFC experimental system with a gross electrical power output of 10 kW, which can exploit the low temperature grade heat by converting it into valuable electricity through an advanced thermal conversion technique referred to as the ocean thermal energy conversion (OTEC) [25,26].

2. Background: ocean thermal energy conversion

The concept of ocean thermal energy conversion was first proposed by D' Arsonval in 1888 [26]. Generally, there is a significant temperature difference between the warm surface seawater (24–30 °C) and the cold seawater at considerable depths (4–8 °C). The vertical temperature distribution in the open ocean naturally forms two enormous thermal reservoirs [27,28]. To make use of the potential thermal energy, a special heat engine is required for such energy conversion [27]. OTEC has become a well-developed technology for ocean thermal resource [26]. It makes use of warm seawater to continuously evaporate a working fluid such as propane or ammonia or the seawater with a low boiling point through the corresponding pressure changes. The vapor produced is used to propel a turbine attached to a generator which produces electricity, and is then condensed back into fluid by cold seawater pumped from the ocean depths [29,30]. Generally, the conversion efficiency of the OTEC is in the range of 2–4% due to the differences in geographic conditions, system sizes, working fluid and the performance of the components [27,30].

2.1. OTEC system configurations

Depending on the cycles used, the OTEC systems can be constructed using open-cycle, closed-cycle or hybrid-cycle configurations [26]. In open-cycle OTEC, flash evaporation is performed in partial vacuum ranging from 3% to 1% atmospheric pressure which is less than the saturation pressure of the warm seawater. When the warm seawater is exposed to this low-pressure environment, it begins to boil and form a large amount of steam which is then used to drive a large turbine. In this process of evaporation, the steam carries away a considerable amount of heat from the liquid phase resulting in a lowering of the seawater temperature and the cessation of boiling. Although only a small fraction (approximately 0.5%) of warm seawater entering the evaporator can be vaporized to be the working fluid and the typical conversion efficiency is less than 3%, the simple structure and the fresh water production make this configuration attractive [27].

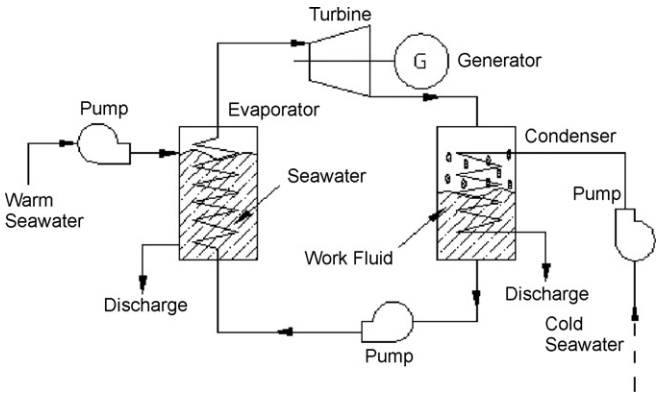

Fig. 1. The schematic diagram of closed-cycle OTEC system.

Unlike the open-cycle OTEC using seawater as the working fluid, closed-cycle OTEC uses some other high vapor density liquid such as freon, propane or ammonia as a secondary working fluid. The evaporation and condensation of the working fluid are performed by the two heat exchangers through which the warm and cold seawater flow respectively [25]. Thus, it overcomes the problem of insufficient density of the steam and improves the efficiency range from 3% to 4% due to a larger enthalpy drop [27]. Moreover, the heavier, higher pressure vapor can be beneficial in that a relatively small turbine can be used to produce electricity in a closed loop, resulting in the smaller system scale and the lower capital cost [31–33].

For hybrid OTEC, the warm seawater is flash-evaporated into steam to produce fresh water, while it also provides heat to vaporize the secondary working fluid through the heat exchanger. Thus hybrid OTEC can have a similar efficiency to that of a closed-cycle system as well as produce desalinated water as in an open-cycle system [26]. Hence, hybrid OTEC combines the benefits of the open-cycle and closed-cycle OTEC configurations. However, the hybrid system is more complicated in configuration and is only at an experimental stage at this time. At the present, only closed-cycle OTEC can achieve economic feasibility compared with other two OTEC configurations [29]. Fig. 1 shows the configuration of a typical closed-cycle OTEC system.

2.2. Limitations of current OTEC systems

Temperature differences between a heat source and a sink on the order of 20 °C for seawater result in low efficiency in Rankine-cycle machines. Considering the conversion efficiency of a turbogenerator, the overall efficiency of an open-cycle OTEC system is not more than 2% in practice [22,34]. Such a meager performance rating requires a considerable parasitic power consumption to maintain the large seawater flow rate ($m^3\,s^{-1}$) for electricity generation [27]. As a result, an OTEC system must generally be large scale, therefore of high capital cost, to ensure sufficient net electrical power output at a cost that is economically competitive with conventional power plants. Moreover, many practical engineering problems including biofouling, corrosion, severe storms and geographical limitation present considerable challenges [35,36]. Nevertheless, many researchers have indicated that the technological challenges of the OTEC may be overcome as a result of the

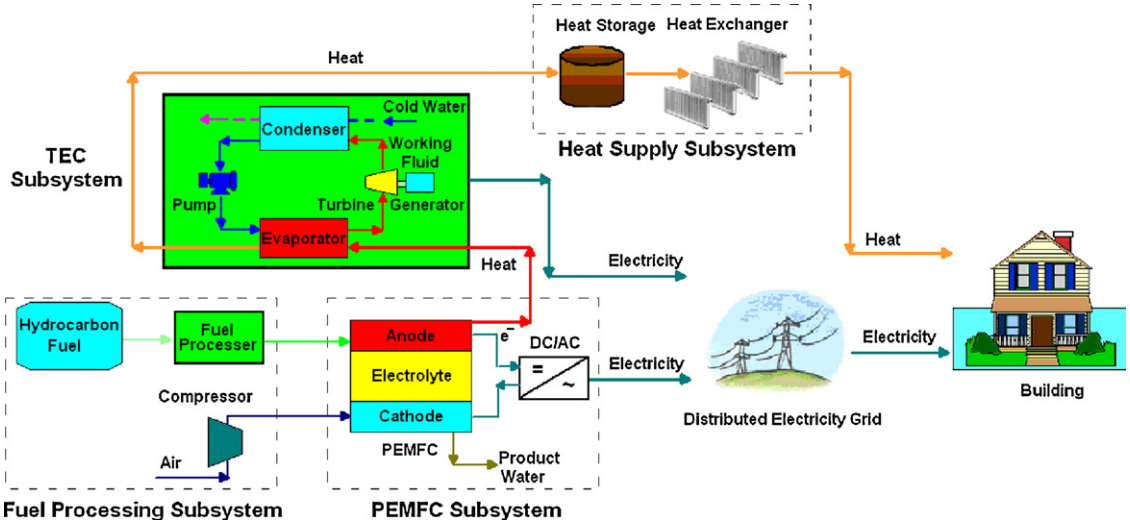

Fig. 2. The configuration of the potential PTEC power plant for the distributed generation.

combination of modern engineering technologies and the increasing investment in recent OTEC projects [1,8].

3. The gradational energy utilization system—PTEC

For any thermal energy conversion (TEC) system, the greater the temperature differences between the heat source and the sink, the greater the power output and generation efficiency [26]. Thus, the PEMFC should be a superior heat source for the TEC system due to the relatively higher quality heat (~60 °C difference between the PEMFC stack and the cold seawater) compared with that of warm surface seawater (~20 °C difference). The heat source with the higher temperature can cause larger enthalpy drop in the working fluid to produce more mechanical work by the turbine. Moreover, redundant heat can still be used to meet heat demand. Through this technology combination, the system achieves the gradational energy utilization for different grade heat to satisfy various energy needs. It would not only improve the overall efficiency of the PEMFC, but also reduce parasitic power consumption, and allow miniaturization for the TEC system. In this paper, a conceptual system combining PEMFC and TEC is an example of a thermally gradational energy utilization system, which will be abbreviated as PTEC.

3.1. System overview

Fig. 2 shows the concept of a future commercial-scale PTEC power plant, which includes four subsystems: (1) the fuel processing subsystem, (2) the PEMFC subsystem, (3) the TEC subsystem and (4) the heat supply subsystem.

Since the fuel reforming process is not considered in this paper, pure hydrogen is used as the fuel of the PEMFC in the later discussion for simplicity. In the PEMFC subsystem, the fuel cell acts as a highly efficient energy conversion device which directly converts the chemical energy of the hydrogen fuel with oxygen to produce electricity, water and heat through the electrochemical reaction [23]. Residual hydrogen that would be incompletely utilized is recovered by the jet pump to refuel the PEMFC. The direct current produced by the fuel cell is converted into alternating current by an inverter, which can be supplied to the local electricity grid. Meanwhile, the fuel cell dissipates heat via its cooling water to a heat exchanger. The captured heat is extracted to generate secondary electricity through the proper thermodynamic cycle in the TEC subsystem, and then the redundant heat in cooling water can still be used to satisfy heat demand such as space and water heating through the existing heat supply network. The remainder of the article focuses on the design specifications and analysis of the PEMFC subsystem and the TEC subsystem.

3.2. Exergy calculation

Exergy indicates the useful part of the total energy in a system not in equilibrium with its reference environment [37], which can be described as:

$$E = (H_1 - H_0) - T_0(S_1 - S_0) \quad (1)$$

where H_i represents the enthalpy, S_i is the entropy and T_0 is the environmental (heat sink) temperature. The exergy loss $\Delta\varepsilon$ can be expressed as [38]:

$$\Delta\varepsilon = T_0\,\Delta S \quad (2)$$

For the PTEC system shown in Fig. 2, exergy analysis is performed to illustrate the process of the energy conversion from the views of the quantity and quality of energy [39]. Table 1 lists the typical parameters of the thermal energy conversion process in such a system.

In the PTEC system, the total energy input E_{total} is evaluated as the product of the mass flow rate q_{fuel} and the enthalpy change ΔH of the fuel.

$$E_{total} = -q_{fuel}\,\Delta H \quad (3)$$

For the fuel cell at 1 at pressure and 60 °C, the change in the reaction enthalpy is about −244 kJ mol^{-1} for gas product water [24].

The energy balance in the PEMFC is derived as follows:

$$E_{total} = W_{FC} + Q_{FC} \quad (4)$$

Table 1
Typical parameters of the process.

Parameter	Property	Value
T_0	Standard environmental temperature	298 K
T_{FC}	Temperature of PEMFC stack	333 K
T_{CW}		
T_H	Intake temperature of hot water pipe	328 K
T_C	Intake temperature of cold water pipe	278 K
T_{wi}	Initial temperature of working fluid	325 K
T_{wf}	Final temperature of working fluid	280 K
η_{FC}	Conversion efficiency of PEMFC	2/5
r_{FC}	The fraction of enthalpy lost from the PEMFC to the environment	1/5
η_{TEC}	Efficiency factor	0.8

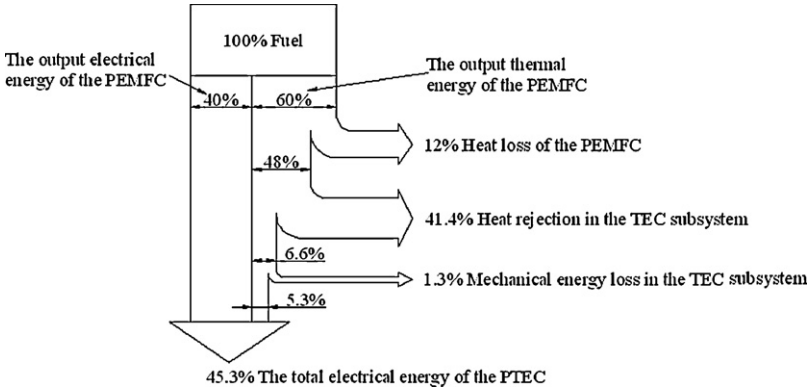

Fig. 3. The distribution of the PTEC energy flow.

Writing the conversion efficiency of the fuel cell as $\eta_{FC} = W_{FC}/E_{total}$, the electrical and thermal energy outputs from the fuel cell are calculated as [40]:

$$W_{FC} = E_{total} \times \eta_{FC} \tag{5}$$

$$Q_{FC} = E_{total} \times (1 - \eta_{FC}) \tag{6}$$

Generally, a PEMFC stack loses some part of its generated heat to the environment by means of convection and radiation. This loss depends on ambient temperature and on the size of the cell stack. For a megawatt scale system, the loss would generally be very small. A PEMFC stack having a voltage rating of 12 V and a power rating of 200 W is used to test the amount of heat loss. The geometric parameters of the stack are 150 mm × 70 mm × 100 mm. Twenty pieces of Nafion 112 membrane with effective area of 32 cm^2 are installed for the stack. According to experimental data, when the cooling water is maintained at a flow rate of 0.15 L min^{-1}, the cell potential is 0.64 V at the current density of 400 mA cm^{-2} and the temperature of 45 °C. Under this condition, when the heat conservation measure is adopted for the stack, the temperature of the cooling water can increase approximately 2.8 °C. Based on the above experimental results, the heat loss can be estimated to be approximately 19% of the total heat, which is closed to the typical value of 20% reported in the literature [15]. Thus, the enthalpy absorbed by the cooling water can be expressed as:

$$Q_{water} = Q_{FC} \times (1 - r_{FC}) \tag{7}$$

where r_{FC} is the fraction of enthalpy lost to the environment.

The exergy loss due to heat rejection from the fuel cell to the cooling water is:

$$\Delta\varepsilon_{water} = T_0 \left(\frac{Q_{water}}{T_{CW}} - \frac{Q_{water}}{T_{FC}} \right) \tag{8}$$

where T_0 is the environmental temperature, T_{CW} is the temperature of the cooling water, and T_{FC} is the temperature of the PEMFC stack.

Thus, the exergy input for the cooling water can be calculated as:

$$E_{water} = Q_{water} \left(1 - \frac{T_0}{T_{CW}} + \frac{T_0}{T_{FC}} \right) \tag{9}$$

Assuming that negligible enthalpy losses occur on heat transfer from the cooling water to the working fluid of the heat engine, the heat $Q_{evaporator}$ obtained by the evaporator can be considered approximately as Q_{water}. For a closed-cycle TEC subsystem, the hot water pipe (HWP) and cold water pipe (CWP) are employed to evaporate and condense the working fluid alternately in a closed loop. The intake temperatures of HWP and CWP are expressed as T_H and T_C, respectively. Here, ΔT represents the temperature difference between T_H and T_C.

When the working fluid absorbs the heat from the HWP and releases it to the CWP, the initial and final temperature of the working fluid can be respectively expressed as [26]:

$$T_{wi} = T_H - dT_H - dT_{w,absorb} \tag{10}$$

$$T_{wf} = T_C + dT_C + dT_{w,release} \tag{11}$$

where $T_{w,absorb}$ and $T_{w,release}$ indicate the temperature of the working fluid in the boundary layer heat transfer process, respectively.

The actual available power output W_{TEC} from the TEC subsystem is

$$W_{TEC} = \eta_{TEC} Q_{evaporator} \left(1 - \frac{T_{wf}}{T_{wi}} \right) \tag{12}$$

where η_{TEC} is the efficiency factor, which is in the range of 0.75–0.85 [26]. Since the entropy intake of the evaporator in this process is

$$S_{evaporator} = \frac{Q_{evaporator}}{T_{wi}} \tag{13}$$

according to Eqs. (10), (11) and (13), the power output can also be expressed as:

$$\begin{aligned} W_{TEC} &= \eta_{TEC} S_{evaporator} (T_{wi} - T_{wf}) = \eta_{TEC} S_{evaporator} \\ &\quad [(T_H - T_C) - d(T_H + T_{w,absorb}) - d(T_C + T_{w,release})] \\ &= \eta_{TEC} S_{evaporator} [\Delta T - d(T_H + T_{w,absorb}) - d(T_C + T_{w,release})] \end{aligned} \tag{14}$$

It may be concluded that the output power of the TEC subsystem is directly proportional to the temperature difference ΔT between the HWP and the CWP. Obviously, more output power can be extracted from the working fluid using a greater temperature differential and with lower heat losses. Thus, compared with warm surface seawater, the PEMFC should be a better heat source to provide heat with the higher temperature to the TEC subsystem. Fig. 3 shows the distribution of the PTEC energy flow according to the typical parameters listed in Table 1.

4. Analyses and results

Fig. 4 shows a conceptual design for the feasibility demonstration of the combined PEMFC and TEC system prototype. The following sections concentrate on the respective investigations for the PEMFC and TEC subsystems which are the keys to the PTEC system operation. In the PEMFC subsystem, the design parameters of the PEMFC stack are shown in Table 2. The electrical load for the PEMFC stack is made up of sixty light bulbs (voltage: 48 V, nominal power: 200 W) in a parallel electrical circuit. The reaction gas is humidified by a dew point humidifier out of the PEMFC

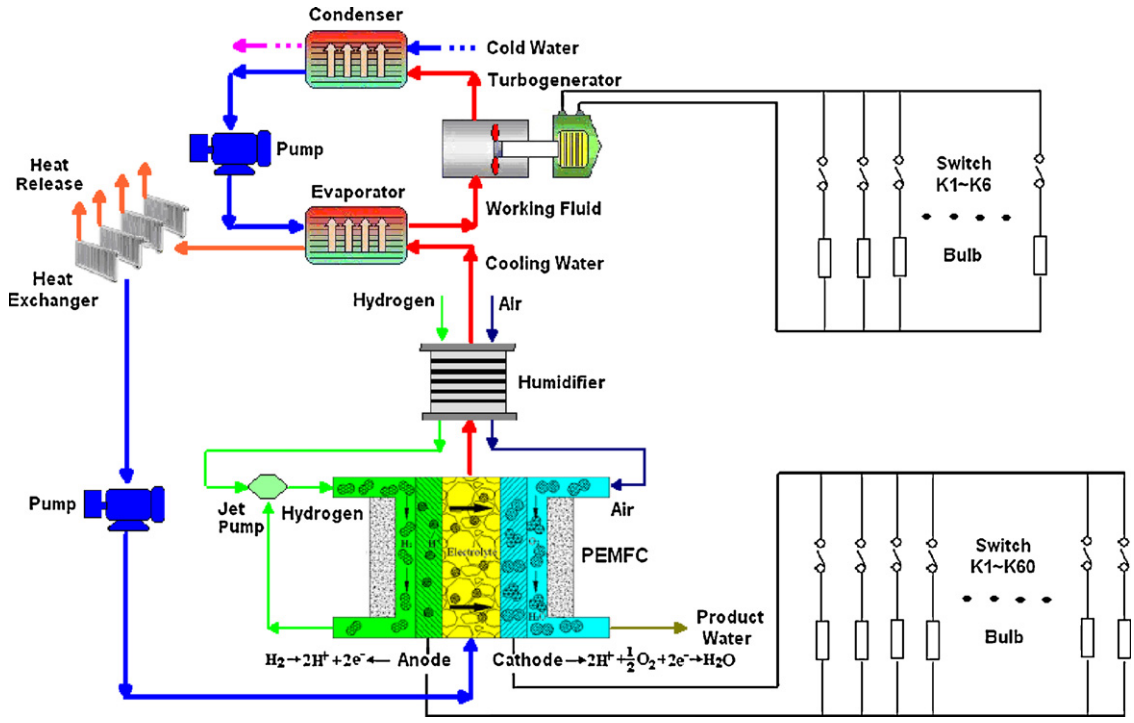

Fig. 4. The process flow diagram for a lab-scale PTEC system prototype.

stack. The hydrogen can be allowed to flow in a recycle loop. The residual hydrogen at the outlet of the PEMFC stack can be pumped back into the inlet by the jet pump powered by the high pressure gas. Twenty cooling cells are inside the stack to capture the heat adequately. Cooling water carries the heat from cooling cells and circulates by a pump in a direction counter to the reaction gas from the anode. Thus, heat produced by the PEMFC is transferred by the heat exchanger to the ammonia which is the working fluid in the closed-cycle TEC subsystem.

The two heat exchangers including the evaporator and condenser are the most expensive components in the TEC subsystem. Considering the heat transfer efficiency and space, a plate heat exchanger with heat transfer area of 2 m^2 is adopted in this lab-scale system. Its geometric parameters are 0.7 m × 0.5 m × 0.3 m. The total cost of the two heat exchangers is about US$ 2500. The liquid ammonia is evaporated into the high density vapor in the evaporator, to drive a miniature turbine to generate electricity at about 2 MPa pressure. The turbine is undoubtedly the most significant component in the TEC subsystem. It has a designed flow rate of 14 kg h^{-1} and costs US$ 1800. After the vapor passes through the turbine, it is condensed back into liquid by the cold water at 5 °C. The liquid ammonia is pumped into the evaporator in a closed loop.

Table 2
Parameters of the PEMFC stack.

Nominal power output	10 kW
Voltage rating	48 V
Proton exchange membrane	Nafion 112
Effective area of the membrane	780 cm^2
Amount of cells	70
Operating temperature	65 °C
Operating pressure	0.1 MPa
Relative humidity of the gas	100%
Fuel	Pure hydrogen
Fuel stoichiometry	1.2
Air stoichiometry	4

4.1. The PEMFC subsystem

In this PTEC system, the PEMFC is the key component acting as the primary electrical and thermal source for the whole system. Since the PEMFC converts chemical energy of the fuel into thermal and electrical energy during the first stage of the energy conversion process, it plays a very significant role in determining the overall performance of the PTEC system. Hence, a PEMFC system with nominal power of 200 W is constructed, as shown in Fig. 5a, to test the electrical and thermal performance of the fuel cell under different operating parameters. Through this real system operation, some important experimental results such as power and heat density can be used to further support the PTEC system feasibility and help design the TEC subsystem to match the future 10 kW PEMFC subsystem.

For a PEMFC, other than inherent qualities depending on materials and manufacture, the operating conditions can also affect its performance to a large extent because they can alter the shape and position of the polarization curve [18]. During the operation, the fuel cell efficiency generally depends on mean cell potential as a function of current density. As current density is changed by load and operation parameters including pressure, relative humidity and stoichiometery, the PEMFC efficiency eventually takes place the corresponding change. Through the analysis of experimental results, a conclusion can be drawn that temperature has a more significant influence in the performance of the PEMFC than other operation variables [41,42]. Fig. 5b shows that the polarization curves of the PEMFC shift upwards as temperature increases from 20 °C to 60 °C under control of the cooling water. This phenomenon indicates the improvement of electrical efficiency as temperature increases. It can be explained in that the rise of the temperature increases proton mobility in the membrane and improves catalyst activity and gas diffusion [42]. A much higher temperature is beneficial for the PEMFC to reduce inner resistance and improve electrical performance. However, according to the experimental data, it can also be concluded that the influence of temperature is limited, the voltage having only

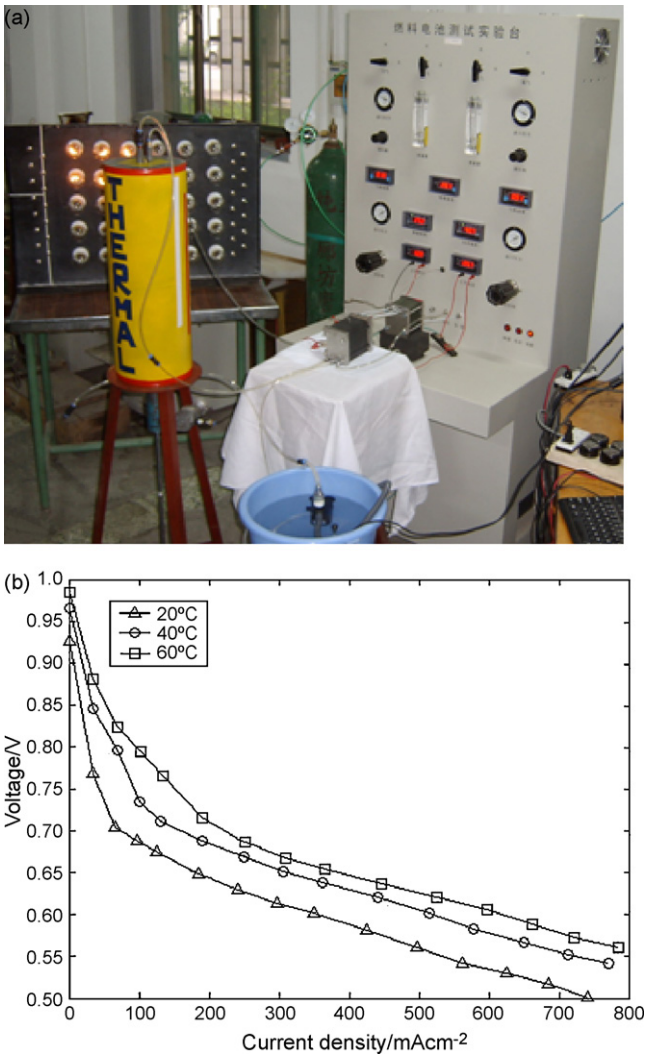

Fig. 5. (a) Electrical and thermal testing for a small PEMFC stack: nominal power: 200 W, nominal voltage: 12 V; (b) polarization curves of a single cell.

a marginal improvement above the temperature of 60 °C. This is because of drying of the membrane and increase in internal resistance. In regard to the durability and life of the PEMFC, thermal management is required to maintain its temperature below 70 °C.

Generally, the temperature of the PEMFC changes as current density increases with no cooling water control, because the heat-to-power ratio also increases as the electrochemical reactions become more irreversible [18,41]. For the utilization of thermal energy by the TEC subsystem under the condition of the variable electrical loads of the PEMFC, it is necessary to determine the change in heat production due to increase of current density or electrical loads. Fig. 6 shows that the surface heat generation rate and the temperature of the PEMFC increase as the current density increases when the cooling water is maintained at a flow rate of 0.15 L min^{-1}. Experimental results show that the surface heat generation rate approximately increases from 0.05 W cm^{-2} to 0.5 W cm^{-2} and the stack temperature rises from 25 °C to 65 °C as the current density increases from 100 mA cm^{-2} to 800 mA cm^{-2}. In each case, the PEMFC will eventually reach equilibrium with its environment as time goes on. On increasing the electrical load, a new equilibrium is reached at a higher temperature due to the higher surface heat generation rate [23,41]. Moreover, most of heat in the fuel cell subsystem is transferred to the cooling water and

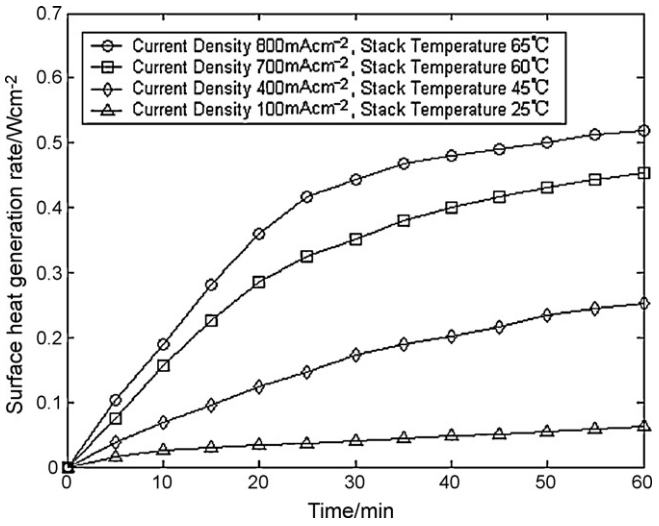

Fig. 6. Surface heat generation rates of a single cell at different current densities.

the increase in water temperature lags behind the increase in stack temperature.

4.2. The TEC subsystem

Performance simulation of a TEC subsystem is performed based on heat supply from a 10 kW PEMFC subsystem whose performance parameters are deduced by the above experiment. Inevitably, as the temperature difference increases, heat exchange and the thermodynamic efficiency of the TEC subsystem also increase. Fig. 6 shows that the stack temperature and current density are interrelated without external temperature control. In the given 10 kW PEMFC system, as the current density increases, more heat is produced and carried to the evaporator by the cooling water at the constant flow rate of 12 L min^{-1}, while more working fluid is evaporated into vapor passing through the turbine. Fig. 7a and b shows the simulation results that the thermodynamic efficiency and the flow rate of the vapor both increase linearly with rising fuel cell temperature whereas turbogenerator efficiency shows a nonlinear characteristic relative to the flow rate of the vapor. Combining Figs. 6 and 7, the thermodynamic efficiency improves approximately from 2.5% to 8.2% and the flow rate of the vapor increases approximately from 230 mL s^{-1} to 840 mL s^{-1} as the temperature of fuel cell rises from 25 °C to 65 °C. This is caused by the increase of current density from 100 mA cm^{-2} to 800 mA cm^{-2}. The operating efficiency of the miniature turbine is reduced when the practical flow rate of the vapor deviates from the design parameter. The main reason is due to a loss in speed due to flow separation on the turbine blades. In other words, the turbine cannot handle the excess vapor for electricity generation [43]. Fig. 7b shows that the maximum turbogenerator efficiency is 72% when the flow rate is 530 mL s^{-1} at the stack temperature of 45 °C. Specially, for a potential high temperature (>95 °C) PEMFC, a larger turbine has to be required to increase the design capacity for the large vapor flow rate as well as to improve the power output and conversion efficiency of the TEC system.

For the TEC subsystem, efficiency is defined as the product of the thermodynamic efficiency and the turbogenerator efficiency. Theoretically, the power output and TEC efficiency should also increase with a rise of fuel cell temperature. In practice, as shown in Fig. 8, TEC thermodynamic efficiency and power output are non-linear functions of fuel cell temperature, however, the respective maximum values do not appear at the same temperature. Generally, the temperature for maximum TEC power output lags a little behind

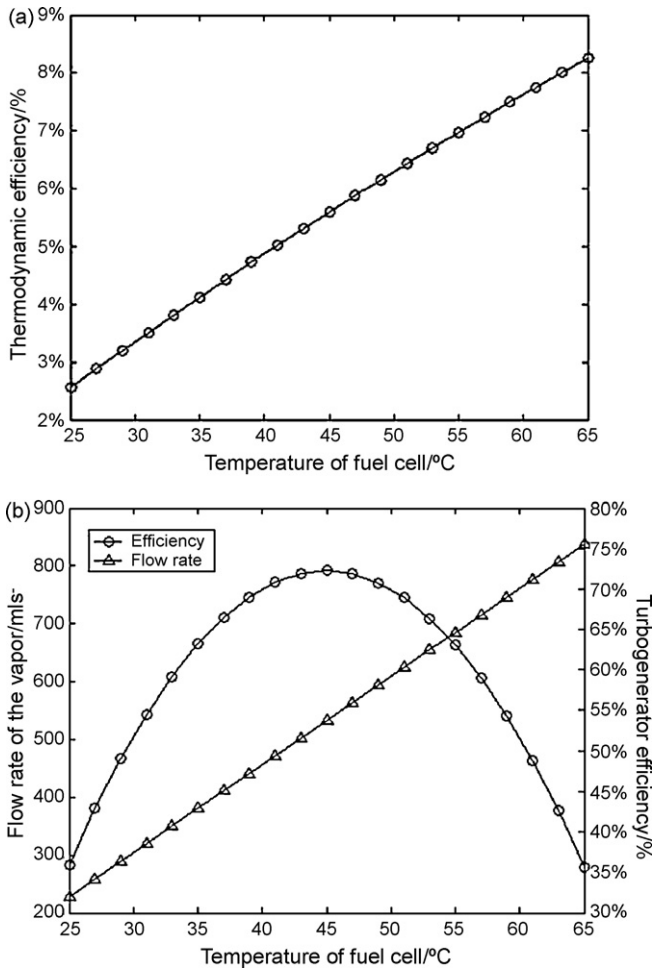

Fig. 7. (a) Thermodynamic efficiency; (b) turbogenerator efficiency and vapor flow rate at different temperatures of the fuel cell stack.

the temperature at the maximum TEC efficiency due to the increasing heat amount from the PEMFC. Fig. 8 shows the maxima are at 58 °C for the maximum power output (311 W) and at 53 °C for the maximum TEC efficiency (4.4%). For a large enough turbine, the turbogenerator efficiency should not be a problem and the TEC efficiency could be improved to 7% by increasing the design capacity for the vapor flow rate.

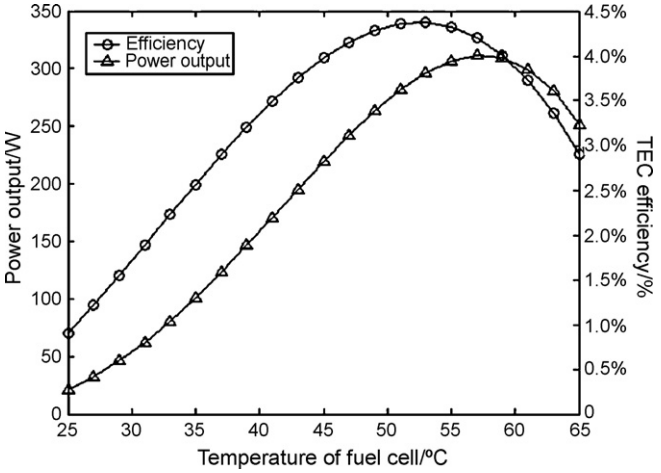

Fig. 8. TEC efficiency and power output of the TEC subsystem.

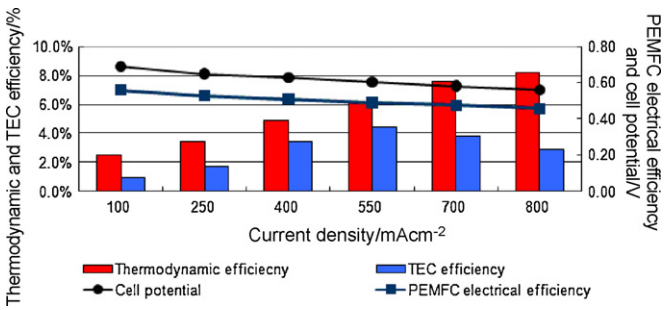

Fig. 9. Efficiency analysis for the PEMFC and the TEC subsystems.

4.3. Efficiency and cost analysis

As shown in Fig. 5b, when the PEMFC operates with a fixed electrical load, the PEMFC can achieve high performance at high temperature under cooling loop control. However, the PEMFC electrical efficiency as a whole still declines because increase in current density increases polarization. Fig. 9 shows that as the current density increases from 100 mA cm^{-2} to 800 mA cm^{-2}, the cell potential declines from 0.69 V to 0.56 V and the electrical efficiency reduces from 56% to 46%. Meanwhile, the thermodynamic efficiency of the TEC subsystem improves from 2.5% to 8.2% when the temperature of the PEMFC is allowed to rise from 25 °C to 65 °C.

Based on energy equilibrium of the PEMFC, the overall efficiency can be calculated as follows:

$$\eta_{\text{overall}} = \eta_{\text{electrical}} + (1 - \eta_{\text{electrical}}) \times \eta_{\text{TEC}} \quad (15)$$

where η_{overall} is the overall efficiency, $\eta_{\text{electrical}}$ is the electrical efficiency of the PEMFC, η_{TEC} is the TEC efficiency. According to Eq. (15) and Fig. 9, the electricity generation of the TEC subsystem contributes to the increase in the overall efficiency in the range 0.4–2.3%. As mentioned above, the maximum TEC efficiency of 4.4% results in the maximum overall efficiency increase of 2.3% when the PEMFC operates at a current density of 550 mA cm^{-2} and at 53 °C.

Although the electrical efficiency of the PEMFC is high at low current densities, overall cost per kW for a commercial PEMFC power plant is also influenced by economic factors, such as the cost of the fuel cell, the life of the membrane and the inflation rate. Generally, the electricity cost of the fuel cell is determined by the capital cost, fuel cost and maintenance cost. In this analysis, the electricity cost can be estimated as follows, assuming negligible maintenance cost [44]:

$$C = \frac{C_{\text{captial}} + C_{\text{fuel}}}{W} \quad (16)$$

where C is the electricity cost (US\$ kW h^{-1}), C_{capital} is annualized capital cost (US\$ yr^{-1}), C_{fuel} is annual fuel cost (US\$ yr^{-1}), W is annual electricity production (kW h yr^{-1}).

The annual electricity production W can be estimated as [44]:

$$W = P \times 8760 \times Z \quad (17)$$

where P is the power output of the fuel cell (kW), Z is the capacity factor which is the ratio of actual energy production and the maximum possible energy output over the same time period (usually one year). Generally, the capital cost is given in terms of annualized capital cost, which can be calculated as [45]:

$$C_{\text{captial}} = \frac{C_{\text{FC}} \times (1+i)^n}{n} \quad (18)$$

where C_{FC} is the cost of the fuel cell system (US\$), i is the average annual inflation rate, n is the life of the fuel cell (year).

Assuming a typical annual inflation rate of $i = 3\%$ and a typical fuel cell life of $n = 5$ years, a total cost of US\$ 36,000 (and US\$

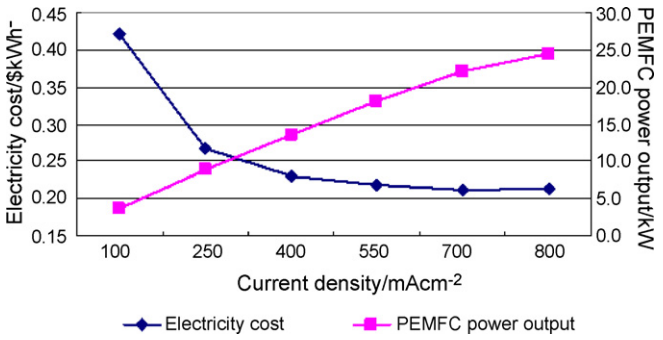

Fig. 10. Changes in electricity cost and power output as a function of current density.

8346 yr^{-1}) for a fuel cell system of nominal power output 10 kW is obtained. The annual fuel cost C_{fuel} can be calculated as [44]:

$$C_{fuel} = C_{hydrogen} \times \frac{W}{\eta_{electrical}} \quad (19)$$

where $C_{hydrogen}$ is hydrogen cost (US$ $kW\,h^{-1}$).

Combining Eqs. (16) and (19), the electricity cost can also be expressed as:

$$C = \frac{C_{captial}}{W} + \frac{C_{hydrogen}}{\eta_{electrical}} \quad (20)$$

Eq. (20) indicates that the electricity cost is a coupling result between current density and electrical efficiency. According to Eqs. (16) and (17), the increase in current density can increase the power output, which results in the reduce in capital cost. On the other hand, operating at a higher current density while reducing the cell potential can have a negative effect on the electrical efficiency of the PEMFC. According to Eq. (19), the reduce of electrical efficiency will cause the increase in fuel cost. Therefore, in the cost analysis, the current density should be carefully selected in order to balance the capital cost and the fuel cost. Assuming market price of hydrogen $C_{hydrogen}$ is US$ 0.07 $kW\,h^{-1}$ and capacity factor Z is estimated to be 0.9, according to Eqs. (16)–(19), Figs. 5 and 6, Table 2, the electricity cost and the power output can be plotted as a function of current density. As shown in Fig. 10, as the current density increases, the power output of the fuel cell increases. The electricity cost rapidly declines due to the reduction in capital cost at the beginning. Above the current density of 700 mA cm^{-2}, the electricity cost curve presents a little rise tendency since the increase in fuel cost counteracts the impact of the reduce of capital cost.

In the current density range of 100–700 mA cm^{-2}, the electricity cost is reduced to US$ 0.22 $kW\,h^{-1}$ when the power output is 17.3 kW at the current density of 520 mA cm^{-2}, after that, there is only a marginal decline in electricity cost as the current density increases. Hence, taking into account the acceptable range of efficiency and related electricity cost, the optimum current density is in the range 520–580 mA cm^{-2}. In this range of current density, the increase in overall efficiency resulting from the TEC cycle is 2.1 to 2.3% from Fig. 9 and Eq. (15), the electricity cost is in the range of US$ 0.22–0.21 $kW\,h^{-1}$ according to Fig. 10. These calculation results show that in this range of current density, the PEMFC can achieve a high overall efficiency and still maintain a low electricity cost.

Well-known OTEC studies estimate the cost of electricity generation for a 10 MW closed-cycle OTEC plant to be approximately US$ 0.14 $kW\,h^{-1}$ where the temperature difference is 20 °C [27,46]. Hence, the generating cost of the TEC system proposed here should be about US$ 0.07 $kW\,h^{-1}$ since such systems have about twice the efficiency (7%) of conventional OTEC as a result of the larger temperature difference.

However, this lab-scale power plant is designed to demonstrate the concept of an integrated PEMFC-TEC in creating an overall hybrid energy conversion technology. Its current scale is too small to be applied for commercial generation because the capital cost of such a TEC system is estimated to be approximately US$ 19,800 kW^{-1}, which is too high to be competitive with conventional electricity production.

5. Conclusion

This paper has demonstrated the feasibility of a gradational thermal energy system named PTEC, which utilizes the heat from the PEMFC to generate secondary electricity by employing the "Ocean Thermal Energy Conversion" technology. Using representative parameters of a PEMFC stack, exergy analysis is performed to illustrate the improvement in the performance of the TEC subsystem by using the comparatively high quality waste heat from the PEMFC. Analytical results show that the PEMFC is a key component which affects the overall performance of the PTEC system. Furthermore, analysis shows that the PEMFC and the TEC subsystems are interrelated through the change of the temperature. When the current density increases from 100 mA cm^{-2} to 800 mA cm^{-2}, the temperature of the PEMFC is increased from 25 °C to 65 °C, while the electrical efficiency of the PEMFC slowly declines from 56% to 46% and the thermodynamic efficiency of the TEC subsystem improves from 2.5% to 8.2%. Specifically, the power output and generating efficiency for the TEC subsystem shows a nonlinear function based on the characteristic of a miniature turbogenerator.

Acknowledgements

The research was supported by National Natural Science Fundation (50835006) of China, by Program for New Century Excellent Talents in Universities (NCET) and by the Research Fund for the Doctoral Program of Higher Education Grant (20050056006) of China. C. Xie' visit to the University of Michigan was supported by China Scholarship Council and the University of Michigan. The authors also greatly acknowledge the constructive feedbacks from anonymous reviewers which helped improve the paper.

References

[1] R. Pelc, R.M. Fujita, J. Marine Policy 26 (2002) 471–479.
[2] C. Flavin, M. O'Meara, Financing Solar Electricity, vol. 10, no. 3, World Watch Magazine, 1997.
[3] US Department of Energy, Annual Energy Outlook 2002 With Projections to 2020, http://www.eia.doe.gov/oiaf/aeo/.
[4] G.C. Nihous, J. Energy Resour. Technol. 129 (2007) 10–17.
[5] M. Granovskii, I. Dincer, M.A. Rosen, J. Power Sources 167 (2007) 461–471.
[6] C. Zener, Phys. Today 26 (1973) 48–53.
[7] C. Zener, Mech. Eng. 99 (12) (1997) 26–29.
[8] R. Gross, M. Leach, A. Bauen, J. Environ. Int. 29 (2003) 105–122.
[9] S.J. Herzog, Appraisal J. 67 (1) (1999) 24–28.
[10] House of Commons, Science and Technology—Seventh Report: Wave and Tidal Energy, London, http://www.parliament.the-stationery-office.co.uk/pa/cm200001/cmselect/cmsctech/291/29102.htm, 2001.
[11] DOE, Federal Energy Management Program, US Department of Energy, Combined Heat and Power: A Federal Manager's Resource Guide (Final Report), 2000.
[12] S.S. Penner, J. Energy 31 (2006) 33–43.
[13] M. Benito, R. Padilla, J.L. Sanz, L. Daza, J. Power Sources 169 (2007) 123–130.
[14] J.M. Ogden, M.M. Steinnbugler, T.G. Kreutz, J. Power Sources 79 (2) (1999) 143–168.
[15] M. Ay, A. Midilli, I. Dincer, Int. J. Energy Res. 30 (2006) 307–321.
[16] W.G. Colella, J. Power Sources 118 (2003) 129–149.
[17] http://ec.europa.eu/research/energy/index_en.htm.
[18] W.G. Colella, J. Power Sources 106 (2002) 388–396.
[19] W.G. Colella, Combined heat and power fuel cell systems, Doctoral Thesis, Transfer Report Department of Engineering Sciences, University of Oxford, Oxford, June 2001.
[20] J. Slowe, All-Energy Conference, International Activity Trends and Strategies in Micro-CHP Systems, Aberdeen, 2006, http://www.all-energy.co.uk/UserFiles/File/Jon_Slowe.pdf.
[21] M.M. Mench, C.Y. Wang, S. Thynell, Int. J. Transport Phenom. 3 (2001) 151–176.
[22] C. Wu, T.J. Burke, J. Appl. Therm. Eng. 18 (5) (1998) 295–300.
[23] G. Hoogers, Fuel Cell Technology Handbook, CRC Press, New York, 2003.

[24] B.L. Yi, Fuel_Cell: Principle. Technique. Application, vol. 1, Chemical Industry Press, Beijing, 2003, pp. 55–56.
[25] M.M. Takahashi, Deep Ocean Water as Our Next Natural Resource, Terra Scientific Publishing Company, Tokyo, 2003, pp. 13–14.
[26] G.T. Heydt, Proc. IEEE 81 (3) (1993) 409–418.
[27] L.A. Vega, J. Marine Technol. Soc. 6 (4) (2002/2003) 25–35.
[28] P. Takahashi, A. Trenka, Ocean Thermal Energy Conversion, Wiley, New York, 1996.
[29] W. Li, Z.N. Zhao, X. Wang, Y.Q. Liu, J. Ocean Eng. 22 (2) (2004) 105–108 (in Chinese).
[30] Z.J. Wu, The Utilization of New and Renewable Energy, vol. 1, China Machine Press, Beijing, 2006, pp. 321–323.
[31] W. Lindenmuth, H. Liu, G. Doquette, Seawater deareration in OC-OTEC risers, Report 8031-1, Hydroraulics, Inc., 1987.
[32] B.K. Parsons, D. Bharathan, J.A. Althof, Thermodynamic systems analysis of open-cycle ocean thermal energy conversion (OTEC), Report SERI/TR-252-2234, 1985.
[33] D. Block, J.A. Valenzuela, Thermoeconomic Optimization of OC-OTEC Electricity and Water Production Plants, Solar Energy Research Institute, Golden, CO, May 1985.
[34] M.T. Pontes, A. Falcao, Ocean Energy Conversion, Lisboa, Portugal, http://www.ebd.lth.se/avd%20ebd/main/summerschool/lectures/lect-p-pontes.pdf, 2007.
[35] D. Tanner, J. Renewable Energy 6 (3) (1995) 367–373.
[36] F.L. La Que, A.H. Tuthill, Trans. Soc. Naval Architects Marine Eng. 69 (1962).
[37] M.M. Hussain, J.J. Baschuk, X. Li, I. Dincer, Int. J. Therm. Sci. 44 (2005) 903–911.
[38] S.E. Wright, J. Renewable Energy 29 (2004) 179–195.
[39] R. Cownden, M. Nahon, M.A. Rosen, Int. J. Exergy 1 (2) (2001) 112–121.
[40] F. Barbir, T. Gomez, Int. J. Hydrogen Energy 22 (1997) 1027–1037.
[41] S.X. Wang, C.G. Xie, Y.H. Wang, L.H. Zhang, W.P. Jie, S.J. Hu, J. Power Sources 169 (2007) 338–346.
[42] L. Wang, A. Hussar, T. Zhou, H. Liu, Int. J. Hydrogen Energy 28 (2003) 1263–1272.
[43] Y.Q. Liu, Theoretical Research on Hybrid Ocean Thermal Energy Conversion System, Master Paper, Department of Mechanical Engineering, Tianjin University, Tianjin, January 2004.
[44] A. Kazim, J. Energy Convers. Manage. 46 (2005) 1073–1081.
[45] http://en.wikipedia.org/wiki/Inflation_rate.
[46] D.E. Lennard, J. Renewable Energy 6 (1995) 359–365.